Bottom strange molecules with isospin 0

Zhi-Feng Sun,[1,*] Ju-Jun Xie,[2,†] and E. Oset[3,‡]

[1]School of Physical Science and Technology, Lanzhou University, Lanzhou 730000, China
[2]Institute of Modern Physics, Chinese Academy of Sciences, Lanzhou 730000, China
[3]Departamento de Fsica Terica and IFIC, Centro Mixto Universidad de Valencia-CSIC, Institutos de Investigacíon de Paterna, Aptdo. 22085, 46071 Valencia, Spain

(Received 26 January 2018; published 31 May 2018)

Using the local hidden gauge approach, we study the possibility of the existence of bottom strange molecular states with isospin 0. We find three bound states with spin parity 0^+, 1^+, and 2^+ generated by the $\bar{K}^*B^*$ and ωB_s^* interaction, among which the state with spin 2 can be identified as $B_{s2}^*(5840)$. In addition, we also study the $\bar{K}^*B$ and ωB_s interaction and find a bound state which can be associated to $B_{s1}(5830)$. In addition, the $\bar{K}B^*$, ηB_s^*, $\bar{K}B$, and ηB_s systems are studied, and two bound states are predicted. We expect that further experiments can confirm our predictions.

DOI: 10.1103/PhysRevD.97.094031

I. INTRODUCTION

The local hidden gauge symmetry was introduced in Refs. [1–4] which regards vector mesons as the gauge bosons and pseudoscalar mesons as the Goldstone bosons. Considering this symmetry together with the global chiral symmetry, one can construct the Lagrangian describing interactions involving vector and pseudoscalar mesons. On the other hand, the Bethe-Salpeter equation is a powerful tool to deal with nonperturbative physics while restoring two-body unitarity in coupled channels. The theory incorporating the above two points has been instrumental in explaining many properties of hadronic resonances. In Ref. [5], the $f_0(1370)$ and $f_2(1270)$ were explained as resonances generated from the $\rho\rho$ interaction. Later, in Ref. [6] the work of Ref. [5] was extended to SU(3), and five of the generated states were identified with the observed $f_0(1370)$, $f_2(1270)$, $f_0(1710)$, $f_2'(1525)$, and $K_2^*(1430)$. In the spin-1 sector, a resonance was also found in Ref. [6] with a mass and width around 1800 and 80 MeV, respectively. This state, $h_1(1800)$, is dynamically generated from the $K^*\bar{K}^*$ interaction, and it was investigated in the process $J/\psi \to \eta K^{*0}\bar{K}^{*0}$ in Ref. [7] and in the process $\eta_c \to \phi K^*\bar{K}^*$ in Ref. [8]. In Ref. [9], the authors studied the interactions of ρ, ω, and D^*, and three states with spin $J = 0$, 1, 2 were predicted, among which the second and third ones were identified with $D^*(2640)$ and $D_2^*(2460)$, respectively. The third state predicted, $D(2600)$, was found later in Ref. [10] and has been reconfirmed [11,12]. This work was extended to the case of the $\rho(\omega)B^*(B)$ interaction in Ref. [13], where $B_1(5721)$ and $B_2^*(5747)$ were explained as $\rho(\omega)B^*$ and ρB molecules.

The first evidence for at least one of the bottom strange states was found by the OPAL experiment [14]. Evidence for a single state interpreted as B_{s2}^* was seen by the Delphi Collaboration [15]. $B_{s2}^*(5840)$ was observed by both the CDF and D0 collaborations in the B^+K^- channel [16–18]. In the CDF experiment, there is another peak in the B^+K^- invariant mass spectrum corresponding to $B_{s1}(5830)$. However, $B_{s1}(5830) \to B^+K^-$ is not allowed. The interpretation is that this peak comes from the channel $B^{*+}K^-$ and B^{*+} decays to $B^+\gamma$ where the photon is not detected. As a consequence, the peak is shifted by the $B^* - B$ mass difference due to the missing momentum of the photon. Recently, the LHCb Collaboration first measured the mass and width of $B_{s2}^*(5840)$ in the $B^{*+}K^-$ channel. In addition, the ratio $\frac{B_{s2}^*(5840)\to B^{*+}K^-}{B_{s2}^*(5840)\to B^+K^-}$ was measured and the decay of $B_{s1}(5830) \to B^{*+}K^-$ was observed as well [19]. In Refs. [20–22], the B_{s0}^* and B_{s1} mesons were explained as $B\bar{K}$ and $B^*\bar{K}$ molecular states, respectively.

In addition, the D0 Collaboration reported the narrow structure $X(5568)$ in the $B_s^0\pi^\pm$ invariant mass spectrum, whose mass and width are $5567.8 \pm 2.9^{+0.9}_{-1.9}$ and $21.9 \pm 0.6^{+5.0}_{-2.5}$ MeV, respectively [23]. However, the LHCb Collaboration [24], CMS Collaboration [25], and CDF Collaboration [26] claimed that no such decay mode was detected. Recently, the D0 Collaboration made further claims for the $X(5568)$ from the decay $X(5568) \to B_s\pi^\pm$

*sunzf@lzu.edu.cn
†xiejujun@impcas.ac.cn
‡Eulogio.Oset@ific.uv.es

and the result is consistent with the previous measurement by the D0 Collaboration [27]. Within various models, many theoretical groups have studied possible ways to explain $X(5568)$ as a tetraquark state, a molecular state, etc. [28–60] (see also the review [61]). In a previous paper [51] we dealt with this problem, concluding that this state could not be interpreted as a molecular state of $B_s\pi$, $B\bar{K}$ and we do not further discuss this issue here.

In this work, we extrapolate the local hidden gauge approach to the systems containing bottom and strange quarks. The paper is organized as follows. After this Introduction, in Sec. II we show the local hidden gauge Lagrangian from which the potentials are obtained. Then, we construct the T matrix by solving the Bethe-Salpeter equation. In Sec. III we present our results. Finally, we conclude with a short summary.

II. FORMALISM

A. Lagrangian

In order to describe the interaction of bottom and strange mesons, we need to use the local hidden gauge approach, under which vector mesons are treated as gauge bosons. The covariant derivative is defined as

$$D_\mu \xi_{L,R} = \partial_\mu \xi_{L,R} - iV_\mu \xi_{L,R}, \tag{1}$$

and the gauge field strength as

$$V_{\mu\nu} = \partial_\mu V_\nu - \partial_\nu V_\mu - ig[V_\mu, V_\nu]. \tag{2}$$

Here, g is given by $g = \frac{m_V}{2f_\pi}$ with the pion decay constant $f_\pi = 93$ MeV, and m_V are the masses of vector mesons. $\xi_{L,R}$ are defined as

$$\xi_L = e^{i\sigma/f_\sigma} e^{-i\frac{1}{\sqrt{2}}P/f_\pi}, \tag{3}$$

$$\xi_R = e^{i\sigma/f_\sigma} e^{i\frac{1}{\sqrt{2}}P/f_\pi}. \tag{4}$$

In this paper, we take the unitary gauge, i.e., $\sigma = 0$. In the above equations, the matrices V_μ and P have the following form:

$$V_\mu = \begin{pmatrix} \frac{\omega}{\sqrt{2}}+\frac{\rho^0}{\sqrt{2}} & \rho^+ & K^{*+} & B^{*+} \\ \rho^- & \frac{\omega}{\sqrt{2}}-\frac{\rho^0}{\sqrt{2}} & K^{*0} & B^{*0} \\ K^{*-} & \bar{K}^{*0} & \phi & B_s^{*0} \\ B^{*-} & \bar{B}^{*0} & \bar{B}_s^{*0} & \Upsilon \end{pmatrix}_\mu ,$$

$$P = \begin{pmatrix} \frac{\eta}{\sqrt{3}}+\frac{\eta'}{\sqrt{6}}+\frac{\pi^0}{\sqrt{2}} & \pi^+ & K^+ & B^+ \\ \pi^- & \frac{\eta}{\sqrt{3}}+\frac{\eta'}{\sqrt{6}}-\frac{\pi^0}{\sqrt{2}} & K^0 & B^0 \\ K^- & \bar{K}^0 & -\frac{\eta}{\sqrt{3}}+\sqrt{\frac{2}{3}}\eta' & B_s^0 \\ B^- & \bar{B}^0 & \bar{B}_s^0 & \eta_b \end{pmatrix}. \tag{5}$$

After defining the blocks

$$\hat{\alpha}_{\perp\mu} = \frac{1}{2i}(D_\mu \xi_R \cdot \xi_R^\dagger - D_\mu \xi_L \cdot \xi_L^\dagger),$$
$$\hat{\alpha}_{\parallel\mu} = \frac{1}{2i}(D_\mu \xi_R \cdot \xi_R^\dagger + D_\mu \xi_L \cdot \xi_L^\dagger), \tag{6}$$

one can construct the Lagrangian [4]

$$\mathcal{L} = \mathcal{L}_A + a\mathcal{L}_V + \mathcal{L}_{III}, \tag{7}$$

where

$$\mathcal{L}_A = f_\pi^2 \langle \hat{\alpha}_{\perp\mu} \hat{\alpha}_\perp^\mu \rangle,$$
$$a\mathcal{L}_V = f_\sigma^2 \langle \hat{\alpha}_{\parallel\mu} \hat{\alpha}_\parallel^\mu \rangle,$$
$$\mathcal{L}_{III} = -\frac{1}{4}\langle V_{\mu\nu} V^{\mu\nu} \rangle, \tag{8}$$

with $f_\sigma^2 = a f_\pi^2$, and we take $a = 2$ as in Ref. [4].

After expanding the Lagrangians in Eq. (7), we get the terms needed in our calculation, i.e., the three-vector vertex

$$\mathcal{L}_{\rm VVV} = ig\langle (\partial_\mu V_\nu - \partial_\nu V_\mu) V^\mu V^\nu \rangle, \tag{9}$$

four-vector vertex

$$\mathcal{L}_{\rm VVVV} = \frac{g^2}{2}\langle V_\mu V_\nu V^\mu V^\nu - V_\nu V_\mu V^\mu V^\nu \rangle, \tag{10}$$

four-pseudoscalar vertex

$$\mathcal{L}_{\rm PPPP} = -\frac{1}{24 f_\pi^2}\langle [P, \partial_\mu P][P, \partial^\mu P] \rangle. \tag{11}$$

and vector-pseudoscalar-pseudoscalar vertex

$$\mathcal{L}_{\rm VPP} = -ig\langle V_\mu [P, \partial^\mu P] \rangle. \tag{12}$$

Note that there is no vector-vector-pseudoscalar-pseudoscalar (VVPP) contact term under the hidden local symmetry. Moreover, since the vector-vector-pseudoscalar interaction is anomalous with a comparatively small contribution, we do not take it into account. In this work, we will study the interaction between bottom and strange mesons, so we extend the SU(3) flavor symmetry to SU(4). Next, we change the form of the three-vector Lagrangian in Eq. (9) through some short calculations,

$$\begin{aligned} \mathcal{L} &= ig\langle (\partial_\mu V_\nu - \partial_\nu V_\mu) V^\mu V^\nu \rangle \\ &= ig\langle V_\mu V_\nu \partial^\mu V^\nu - V_\mu \partial^\mu V^\nu V_\nu \rangle \\ &= ig\langle V_\mu [V_\nu, \partial^\mu V^\nu] \rangle, \end{aligned} \tag{13}$$

from which we see that this Lagrangian has a similar form as that in Eq. (12) except for the minus sign.

As noted in Ref. [62], for small three-momenta of the vector mesons compared to their mass, the ϵ^0 component of the external vectors can be neglected. V_μ in the last line of Eq. (13) cannot correspond to an external vector. If this were the case, ν would be spatial and ∂^i $(i = 1, 2, 3)$ would lead to negligible three-momenta of vector mesons. Then, the Lagrangian in Eq. (13) would give zero contribution. Henceforth, we conclude that V_μ in Eq. (13) corresponds to the exchange vector. Similarly, in Eq. (12), V_μ corresponds to the exchanged vector too. So Eqs. (13) and (12) are formally identical, except for an additional factor $\vec{\epsilon}\cdot\vec{\epsilon}$ which comes from $V_\nu V^\nu$ (note that $\epsilon_\mu\epsilon^\mu$ gives $-\vec{\epsilon}\cdot\vec{\epsilon}$).

It should be noted that the local hidden gauge approach is constructed within SU(2) or SU(3) [63,64]. In the heavy-quark sector one cannot invoke heavy mesons as Goldstone bosons. Yet, the extension to the heavy-quark sector is possible because the dominant terms of the interaction correspond to the exchange of light vectors (ρ, ω, ϕ) and the heavy quarks of the hadrons are just spectators. In this case it is possible to make a mapping of the interaction in the heavy-light hadron sector to the one in the heavy hadron sector. For practical purposes one can use the local hidden gauge Lagrangians extrapolated to SU(4) as in Eq. (5), since for the exchange of light vectors one is only making use of the relevant SU(3) subgroup. Discussions on this issue and the proof of this property can be seen in Sec. II of Ref. [65] and Sec. II and the Appendix of Ref. [66].

B. B^* and $\bar{K}^*$ interaction

The interaction terms of $\bar{K}^*B^*$ and ωB_s^* are depicted by the diagrams in Fig. 1, including contact terms and t-channel diagrams. Here, we neglect the bottom-meson-exchange diagrams, which have a much smaller contribution due to the heavy mass of bottom mesons. Besides, the amplitude of $\omega B_s^* \to \omega B_s^*$ is zero, because of the Okubo-Zweig-Iizuka (OZI) rule [67–69]. Recalling the isospin doublet (K^{*+}, K^{*0}), $(\bar{K}^{*0}, -K^{*-})$, (B^{*+}, B^{*0}), $(\bar{B}^{*0}, -B^{*-})$, and the isospin triplet $(-\rho^+, \rho^0, \rho^-)$, we have the flavor wave functions

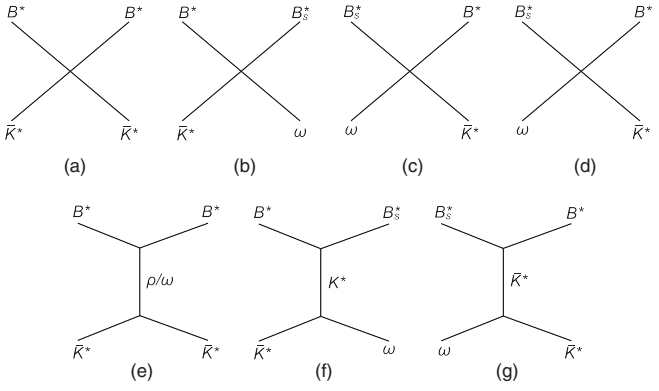

FIG. 1. Feynman diagrams describing the $\bar{K}^*B^*$ and ωB_s^* interaction. (a), (b), (c) and (d) correspond to contact terms, and (e), (f) and (g) are t-channel diagrams.

$$|\bar{K}^*B^*; I = 0\rangle = \frac{K^{*-}B^{*+} + \bar{K}^{*0}B^{*0}}{\sqrt{2}}, \tag{14}$$

$$|\omega B_s^*; I = 0\rangle = \omega B_s^*. \tag{15}$$

Here the channel ϕB_s^* is not considered, since its threshold is much higher than those of the other two. With the structure of Eqs. (12) and (13), all of the amplitudes have the structure $(k_1 + k_3)\cdot(k_2 + k_4)\epsilon_{\mu 1}\epsilon_3^\mu\epsilon_{\nu 2}\epsilon_4^\nu$. As mentioned above, since the three-momenta of the external particles are much smaller than the masses, the ϵ^0 component of the external vector mesons can be neglected. So we have $\epsilon_{\mu 1}\epsilon_{\nu 2}\epsilon_3^\mu\epsilon_4^\nu \sim \epsilon_{i1}\epsilon_{j2}\epsilon_3^i\epsilon_4^j$, $\epsilon_{\mu 1}\epsilon_2^\mu\epsilon_{\nu 3}\epsilon_4^\nu \sim \epsilon_{i1}\epsilon_2^i\epsilon_{j3}\epsilon_4^j$, $\epsilon_{\mu 1}\epsilon_{\nu 2}\epsilon_3^\nu\epsilon_4^\mu \sim \epsilon_{i1}\epsilon_{j2}\epsilon_3^j\epsilon_4^i$, with $i = 1, 2, 3$. After writing the amplitudes using Feynman rules, we project the polarization vector products into different spin states:

$$\mathcal{P}(0) = \frac{1}{3}\epsilon^i\epsilon^i\epsilon^j\epsilon^j, \tag{16}$$

$$\mathcal{P}(1) = \frac{1}{2}(\epsilon^i\epsilon^j\epsilon^i\epsilon^j - \epsilon^i\epsilon^j\epsilon^j\epsilon^i), \tag{17}$$

$$\mathcal{P}(2) = \frac{1}{2}(\epsilon^i\epsilon^j\epsilon^i\epsilon^j + \epsilon^i\epsilon^j\epsilon^j\epsilon^i) - \frac{1}{3}\epsilon^i\epsilon^i\epsilon^j\epsilon^j, \tag{18}$$

where the order of the ϵ's is 1, 2, 3, 4 for the reaction $1 + 2 \to 3 + 4$. Hence, the amplitudes of different spins for $\bar{K}^*B^* \to \bar{K}^*B^*$ (with $I = 0$) are

$$t_{\rm cont}^{S=0} = 4g^2, \tag{19}$$

$$t_{\rm cont}^{S=1} = 6g^2, \tag{20}$$

$$t_{\rm cont}^{S=2} = -2g^2, \tag{21}$$

$$t_{\rm ex}^{S=0,1,2} = -\frac{g^2}{2}\left(\frac{3}{m_\rho^2} + \frac{1}{m_\omega^2}\right)(s - u), \tag{22}$$

and those for $\bar{K}^*B^* \to \omega B_s^*$ are

$$t_{\rm cont}^{S=0} = -4g^2, \tag{23}$$

$$t_{\rm cont}^{S=1} = 0, \tag{24}$$

$$t_{\rm cont}^{S=2} = 2g^2, \tag{25}$$

$$t_{\rm ex}^{S=0,1,2} = \frac{g^2}{m_{K^*}^2}(s - u). \tag{26}$$

In the above equations, the Mandelstam variables s and u are defined as

$$s = (k_1 + k_2)^2, \tag{27}$$

$$u = (k_1 - k_4)^2. \tag{28}$$

C. $B\bar{K}^*$ and $B^*\bar{K}$ interactions

In Fig. 2, we show the diagrams for the $\bar{K}^*B$ and ωB_s interaction. Note that under hidden local symmetry, there is no contact term for vector-pseudoscalar scattering. The amplitude of $\omega B_s \to \omega B_s$ is zero, because of the OZI rules.

For $\bar{K}^*B \to \bar{K}^*B$ with $I = 0$ we need the exchange of ρ and ω, and we obtain

$$t_{\rm ex}^{S=1} = -\frac{g^2}{2}\left(\frac{3}{m_\rho^2} + \frac{1}{m_\omega^2}\right)(s-u) \tag{29}$$

and for $\bar{K}^*B \to \omega B_s$

$$t_{\rm ex}^{S=1} = \frac{g^2}{m_{K^*}^2}(s-u). \tag{30}$$

Similarly, we can also get the amplitudes for the $\bar{K}B^* \to \bar{K}B^*$ process with $I = 0$ as follows:

$$t_{\rm ex}^{S=1} = -\frac{g^2}{2}\left(\frac{3}{m_\rho^2} + \frac{1}{m_\omega^2}\right)(s-u). \tag{31}$$

However, according to the diagrams shown in Fig. 3, the calculation for $\bar{K}B^* \to \eta B_s^*$ with $I = 0$ is a little bit different. Using the Feynman rules and considering the flavor wave function, we obtain

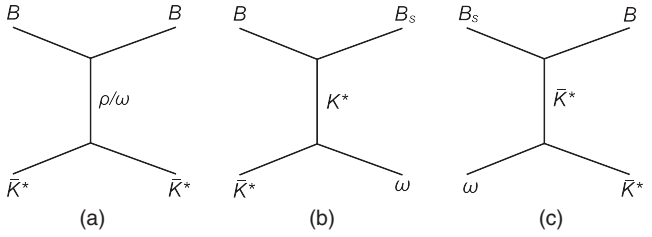

FIG. 2. Feynman diagrams describing the $\bar{K}^*B$ and ωB_s interaction. (a), (b) and (c) correspond to ρ/ω, K^* and $\bar{K}^*$ exchange, respectively.

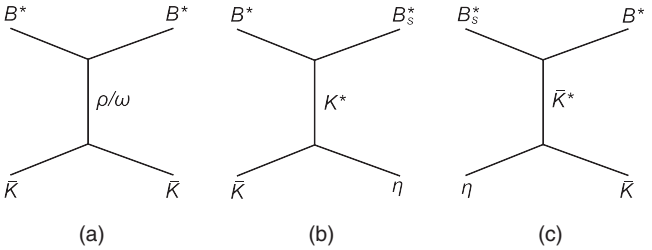

FIG. 3. Feynman diagrams describing the $\bar{K}B^*$ and ηB_s^* interaction. (a), (b) and (c) correspond to ρ/ω, K^* and $\bar{K}^*$ exchange, respectively.

$$t_{\rm ex}^{S=1} = -\frac{2\sqrt{6}g^2}{3m_{K^*}^2}(s-u). \tag{32}$$

D. B and $\bar{K}$ interaction

In Fig. 4, we show the diagrams depicting the interaction of pseudoscalar and pseudoscalar mesons. The amplitude of the contact terms corresponding to Eq. (11) for the $\bar{K}B \to \bar{K}B$ process with $I = 0$ are

$$t_{\rm cont}^{S=0} = -\frac{1}{6f^2}(2u - t - s), \tag{33}$$

those for the $\bar{K}B \to \eta B_s$ process are

$$t_{\rm cont}^{S=0} = -\frac{\sqrt{6}}{12f^2}(s-u), \tag{34}$$

and those for the $\eta B_s \to \eta B_s$ process are

$$t_{\rm cont}^{S=0} = -\frac{1}{36f^2}(-2t + u + s), \tag{35}$$

with $t = (k_1 - k_3)^2$. The amplitudes of t-channel diagrams for $\bar{K}B \to \bar{K}B$ are

$$t_{\rm ex}^{S=0} = -\frac{g^2}{2}\left(\frac{3}{m_\rho^2} + \frac{1}{m_\omega^2}\right)(s-u), \tag{36}$$

and those for $\bar{K}B \to \eta B_s$ are

$$t_{\rm ex}^{S=1} = -\frac{2\sqrt{6}g^2}{3m_{K^*}^2}(s-u). \tag{37}$$

The t-channel diagrams for $\eta B_s \to \eta B_s$ give zero contribution.

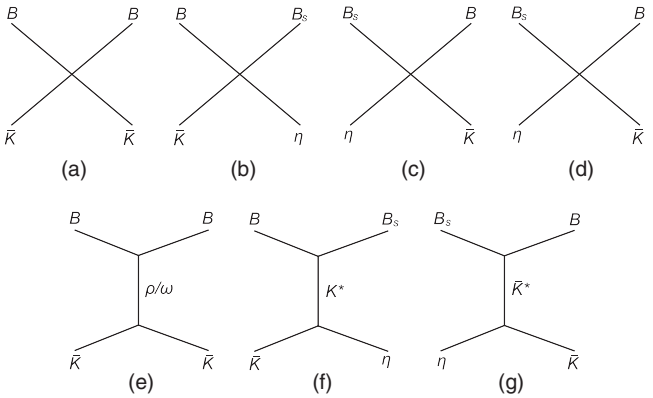

FIG. 4. Feynman diagrams describing the $\bar{K}B$ and ηB_s interaction. (a), (b), (c) and (d) correspond to contact terms, and (e), (f) and (g) are t-channel diagrams.

E. T matrix

With the preparation above, using the Bethe-Salpeter equation in its on-shell factorized form, we obtain the T matrix

$$T = (I - VG)^{-1}V, \tag{38}$$

where V corresponds to the transition amplitudes shown above, but projected to the s wave. So we neglect the product $\vec{k}_1 \cdot \vec{k}_3$ in the Mandelstam variables u and t which corresponds to the p-wave contribution, i.e.,

$$\begin{aligned} u &\approx \frac{m_1^2 + m_2^2 + m_3^2 + m_4^2}{2} - \frac{(m_4^2 - m_3^2)(m_1^2 - m_2^2)}{2s}, \\ t &\approx \frac{m_1^2 + m_2^2 + m_3^2 + m_4^2}{2} + \frac{(m_4^2 - m_3^2)(m_1^2 - m_2^2)}{2s}. \end{aligned} \tag{39}$$

G is the two-meson loop function

$$G = i \int \frac{d^4q}{(2\pi)^4} \frac{1}{q^2 - m_1^2 + i\epsilon} \frac{1}{(P-q)^2 - m_2^2 + i\epsilon}. \tag{40}$$

Using a cutoff for the three-momentum, we have

$$G = \int_0^{q_{\max}} \frac{q^2 dq}{(2\pi)^2} \frac{\omega_1 + \omega_2}{\omega_1 \omega_2 [(P^0)^2 - (\omega_1 + \omega_2)^2 + i\epsilon]}. \tag{41}$$

This integral was already done (see Ref. [70]), and we show it as follows:

$$\begin{aligned} G = \frac{1}{32\pi^2} \Bigg[\frac{\nu}{s} \Bigg\{ \log \frac{s - \Delta + \nu\sqrt{1 + \frac{m_1^2}{q_{\max}^2}}}{-s + \Delta + \nu\sqrt{1 + \frac{m_1^2}{q_{\max}^2}}} + \log \frac{s + \Delta + \nu\sqrt{1 + \frac{m_1^2}{q_{\max}^2}}}{-s - \Delta + \nu\sqrt{1 + \frac{m_1^2}{q_{\max}^2}}} \Bigg\} - \frac{\Delta}{s} \log \frac{m_1^2}{m_2^2} \\ + 2\frac{\Delta}{s} \log \frac{1 + \sqrt{1 + \frac{m_1^2}{q_{\max}^2}}}{1 + \sqrt{1 + \frac{m_2^2}{q_{\max}^2}}} + \log \frac{m_1^2 m_2^2}{q_{\max}^4} - 2 \log \left[\left(1 + \sqrt{1 + \frac{m_1^2}{q_{\max}^2}} \right) \left(1 + \sqrt{1 + \frac{m_2^2}{q_{\max}^2}} \right) \right] \Bigg]. \end{aligned} \tag{42}$$

In Eqs. (40)–(42), P is the total four-momentum of the two mesons in the loop, m_1 and m_2 are the masses, $q_{\max}$ stands for the cutoff, $\omega_i = \sqrt{\vec{q}_i^2 + m_i^2}$, P^0 is nothing but the center-of-mass energy $\sqrt{s}$, $\Delta = m_2^2 - m_1^2$, and $\nu = \sqrt{[s - (m_1 + m_2)^2][s - (m_1 - m_2)^2]}$.

III. RESULTS

A. Discussion of the couplings under SU(4) symmetry

In this subsection, we follow Refs. [13,65,71] and discuss the couplings in the Lagrangian. As an example, we consider the vertex of $B^*B^*\rho$. In order to estimate the corresponding coupling, we need to compare this vertex with that of $K^*K^*\rho$, since their topology is the same if the $\bar{s}$ and $\bar{b}$ quarks are seen as spectators. Figure 5 shows the diagrams for these two vertices at the quark level, in which case the corresponding S matrices should be the same, i.e.,

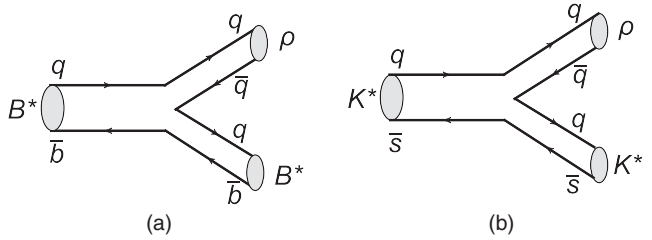

FIG. 5. The vertexes of $B^*B^*\rho$ and $K^*K^*\rho$ at the quark level, which correspond to (a) and (b), respectively.

$$S^{\text{mic}} = 1 - it\sqrt{\frac{2m_L}{2E_L}}\sqrt{\frac{2m_L'}{2E_L'}}\sqrt{\frac{1}{2\omega_\rho}}\frac{1}{\mathcal{V}^{3/2}}(2\pi)^4\delta(P_{\text{in}} - P_{\text{out}}). \tag{43}$$

On the other hand, at the hadronic level, the S matrices are written as

$$S_{B^*}^{\text{mac}} = 1 - it_{B^*}\frac{1}{\sqrt{2\omega_{B^*}}}\frac{1}{\sqrt{2\omega_{B^*}}}\frac{1}{\sqrt{2\omega_\rho}}\frac{1}{\mathcal{V}^{3/2}}(2\pi)^4\delta(P_{\text{in}} - P_{\text{out}}), \tag{44}$$

$$S_{K^*}^{\text{mac}} = 1 - it_{K^*}\frac{1}{\sqrt{2\omega_{K^*}}}\frac{1}{\sqrt{2\omega_{K^*}}}\frac{1}{\sqrt{2\omega_\rho}}\frac{1}{\mathcal{V}^{3/2}}(2\pi)^4\delta(P_{\text{in}} - P_{\text{out}}). \tag{45}$$

As discussed above, we should have $S_{B^*}^{\text{mac}} = S_{K^*}^{\text{mac}}$ which tells us that the corresponding T matrices obey the following relation at the threshold:

$$\frac{t_{B^*}}{t_{K^*}} = \frac{m_{B^*}}{m_{K^*}}. \tag{46}$$

If we use the Lagrangian in Eq. (9) and calculate the T matrices of the processes in Fig. 5, we find that Eq. (46) holds automatically when the ρ is the exchanged (virtual) vector meson, because the amplitude has the $\partial^\mu \cong \partial^0$ operator acting on the external vectors. The coupling of $B^*B^*\rho$ in Eq. (9) correctly implements the field correction factor of Eq. (46). Since in this case the b quark acts as a spectator in the vertex, this amplitude is automatically consistent with heavy-quark spin symmetry [72]. Similar discussions can be applied to the $BB\rho$ vertex with respect to $KK\rho$, and we have

$$\frac{t_B}{t_K} = \frac{m_B}{m_K}, \tag{47}$$

but this is what we obtain from Eq. (12) using SU(4) flavor symmetry. Effectively one is using SU(3) when the heavy quark is considered as a spectator. In summary, we apply the Lagrangians of Sec. II A, and this automatically takes into account all the elements discussed above.

B. The $\bar{K}^*B^*$ system

With the potentials given in the previous section, we solve the Bethe-Salpeter equation considering the $\bar{K}^*B^*$, ωB_s^*, and ϕB_s^* coupled channels. We also obtain three bound states with $J = 0$, 1, 2, using the cutoff $q_{\max}$ around 1055–1085 MeV. The obtained mass is 5847.8–5831.7 MeV for the spin-2 state which is consistent with that of $B_{s2}^*(5840)$. With this $q_{\max}$, we predict that the bound state with $J = 0$ has a mass of 5908.5–5894.4 MeV, and the one with $J = 1$ has a mass of 5912.1–5898.2 MeV. In Fig. 6, we plot the line shape of the mass distribution of these three states. The Particle Data Group (PDG) [73] reports that the mass of $B_{s1}(5830)$ with spin 1 is smaller than that of $B_{s2}^*(5840)$. However, the generated bound state with spin 1 has a mass about 65 MeV larger than that of the bound state with spin 2. Henceforth, it is difficult to explain the $B_{s1}(5830)$ as the $\bar{K}^*B^*$ bound state. In the next subsection, we will come back to this problem.

The T matrix close to a pole behaves like

$$T_{ij} \approx \frac{g_i g_j}{z - z_R}, \tag{48}$$

where i, $j = \bar{K}^*B^*$, ωB_s^*, ϕB_s^*, g_i is the coupling to the channel i, $\mathrm{Re}(z_R)$ gives the mass of the bound state, $\mathrm{Im}(z_R)$

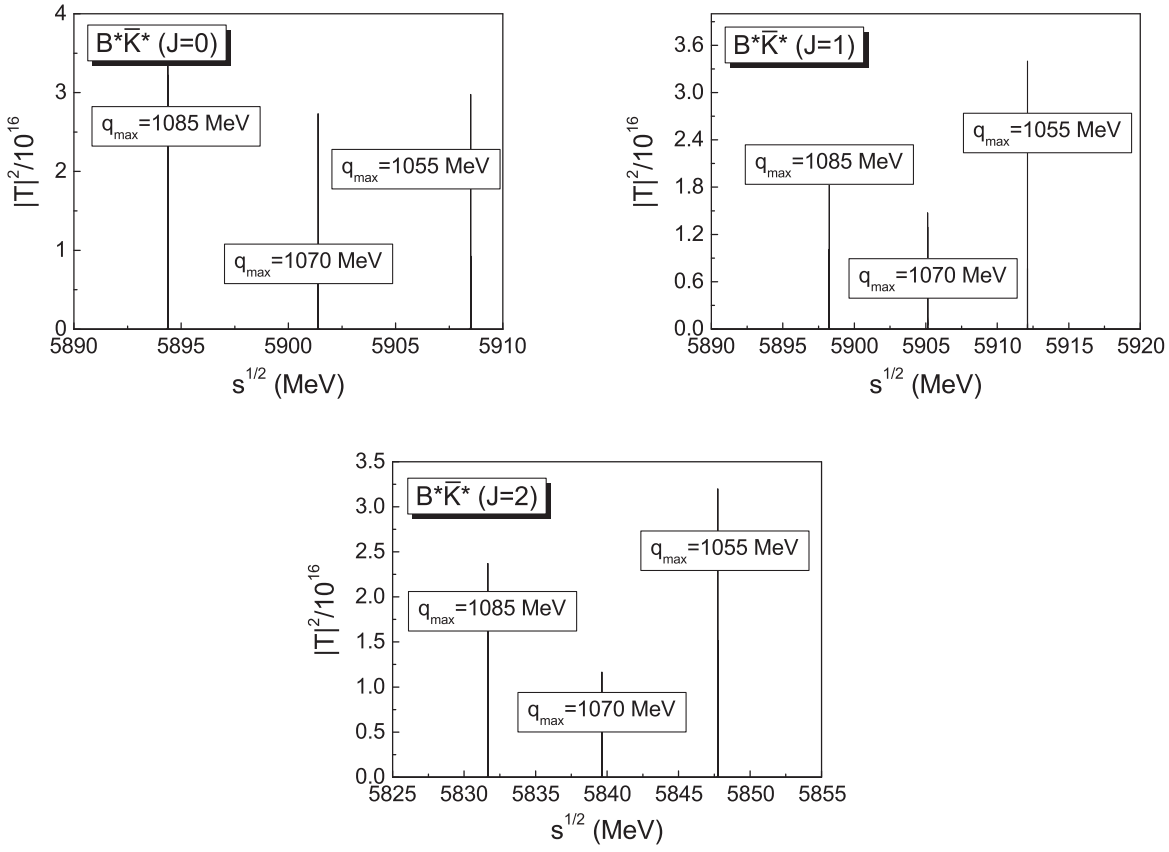

FIG. 6. Squared amplitude for $\bar{K}^*B^*/\omega B_s^*/\phi B_s^*$ systems with spin 0, 1, and 2, respectively.

TABLE I. The couplings for $\bar{K}^*B^*$ systems mixing with ωB_s^*, ϕB_s^* channels. Here we chose the typical value of the cutoff as 1070 MeV. All values are given in units of MeV.

Channel	$J=0$	$J=1$	$J=2$
$\bar{K}^*B^*$	45 955	45 070	49 633
ωB_s^*	−10 696	−14 810	−15 017
ϕB_s^*	18 614	15 702	19 409

gives the half width, and z is the complex value of the Mandelstam variable s. The coupling for a certain channel is obtained as

$$g_i^2 = \lim_{z\to z_R} T_{ii}(z - z_R). \tag{49}$$

The sign of the coupling to the $B^*\bar{K}^*$ channel is chosen as positive, and those for the other channels are then determined by the following formula:

$$\frac{g_i}{g_j} = \lim_{z\to z_R} \frac{T_{ii}}{T_{ij}}. \tag{50}$$

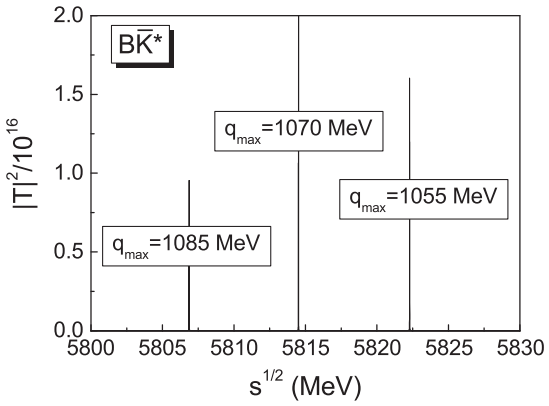

FIG. 7. Squared amplitude for the $\bar{K}^*B/\omega B_s/\phi B_s$ sector depending on the center-of-mass energy.

The value of the couplings are listed in Table I, from which we can see that the $\bar{K}^*B^*$ component is dominant for all of the states.

C. The $\bar{K}^*B$ system

As mentioned in the previous subsection, the $B_{s1}(5830)$ cannot be explained as the $\bar{K}^*B^*$ bound state with spin 1, since in the PDG the mass of $B_{s1}(5830)$ is smaller than that of $B_{s2}^*(5840)$, which is contrary to our results. Now we will try to explain the $B_{s1}(5830)$ under the $\bar{K}^*B/\omega B_s$ system.

Under hidden local symmetry there are no contact terms for the VVPP vertex, so only vector-exchange diagrams are involved. For the vector-exchange terms, the interactions we study in this subsection have the same form as that of the $\bar{K}^*B/\omega B_s/\phi B_s$ interactions. So here we expect to find a bound state like in the case of the $\bar{K}^*B^*$ system. We use $q_{\rm max} = 1055$–1085 MeV fixed in the case of the $\bar{K}^*B^*$ bound state with spin 2. Then we obtain a pole position in the range 5822.3–5806.9 MeV, which is consistent with the mass of $B_{s1}(5830)$ in the PDG. In Fig. 7, we plot the line shape of $|T|^2$ depending on the center-of-mass energy $\sqrt{s}$. We also calculate the couplings, which have the values $g_{\bar{K}^*B} = 47\,654$, $g_{\omega B_s} = -13\,388$, and $g_{\phi B_s} = 18\,855$ with the cutoff $q_{\rm max} = 1070$ MeV.

D. Other predictions

In this subsection, we will show the results corresponding to $\bar{K}B^*/\eta B_s^*$ and $\bar{K}B/\eta B_s$ interactions.

Like the case of the $\bar{K}^*B/\omega B_s/\phi B_s$ system, there are no contact terms for the $\bar{K}B^*/\eta B_s^*$ interaction. Only the vector-meson exchange diagrams are considered. In Fig. 8, we plot the squared amplitude depending on the center-of-mass energy $\sqrt{s}$. Here, we also use the cutoff $q_{\rm max} = 1055$–1085 MeV as before. The pole position is located at 5671.2–5663.6 MeV. The couplings of $B^*\bar{K}$ and $B_s^*\eta$ are 30 637 and −13 919 MeV, respectively, where we choose the cutoff as 1070 MeV.

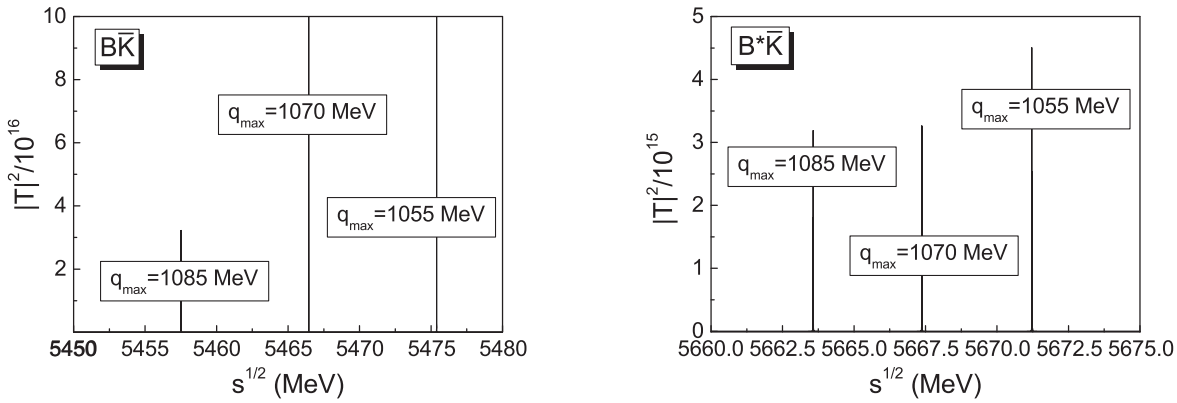

FIG. 8. Squared amplitude for the $\bar{K}B/\eta B_s$ and $\bar{K}B^*/\eta B_s^*$ sector.

TABLE II. Summary of our results where the cutoff is in the range 1055–1085 MeV. Masses in this table are in units of MeV.

State mass	$I(J^p)$	Main component	Experiment	State mass	$I(J^p)$	Main component	Experiment
5475.4–5457.5	$0(0^+)$	$\bar{K}B$	⋯	5908.5–5894.4	$0(0^+)$	$\bar{K}^*B^*$	⋯
5671.2–5663.6	$0(1^+)$	$\bar{K}B^*$	⋯	5912.1–5898.2	$0(1^+)$	$\bar{K}^*B^*$	⋯
5822.3–5806.9	$0(1^+)$	$\bar{K}^*B$	$B_{s1}(5830)$	5847.8–5831.7	$0(2^+)$	$\bar{K}^*B^*$	$B^*_{s2}(5840)$

For the $\bar{K}B/\eta B_s$ system, we predict a bound state with a mass of 5475.4–5457.5 MeV, and the couplings $g_{\bar{K}B} = 53\,577$ MeV and $g_{\eta B_s} = -3689$ MeV, with a cutoff $q_{\max} = 1070$ MeV.

We list our results for all of the systems in Table II.

IV. SUMMARY

In this work, we have studied the systems containing bottom and strange quarks using the chiral unitary approach. Considering $\bar{K}^*B^*$ and ωB_s^* coupled channels and solving the Bethe-Salpeter equation, we found three states with masses 5908.5–5894.4, 5912.1–5898.2, and 5847.8–5831.7 MeV, with the cutoff $q_{\max}$ chosen as 1055–1085 MeV. The state with spin 2 can be identified with $B^*_{s2}(5840)$. From the couplings that we obtained, we can see that the $\bar{K}^*B^*$ component is dominant. However, the $B_{s1}(5830)$ cannot be explained as the state with spin 1, since its mass is smaller than that of $B^*_{s2}(5840)$. So we studied another system, i.e., the $\bar{K}^*B/\omega B_s$ system, and we found a bound state with a mass 5822.3–5806.9 MeV which agrees with the mass of $B_{s1}(5830)$. In addition, we also studied $\bar{K}B^*/\eta B_s^*$ and $\bar{K}B/\eta B_s$ interactions, and predicted two bound states with masses 5671.2–5663.6 and 5475.4–5457.5 MeV, respectively. We expect further experiments to confirm our predictions.

ACKNOWLEDGMENTS

This work is partly supported by the National Science Foundation for Young Scientists of China under Grants No. 11705069 and the Fundamental Research Funds for the Central Universities. It is partly supported by the National Natural Science Foundation of China (Grants No. 11475227 and No. 11735003) and the Youth Innovation Promotion Association CAS (No. 2016367). This work is also partly supported by the Spanish Ministerio de Economia y Competitividad and European FEDER funds under the Contract No. FIS2011-28853-C02-01, No. FIS2011- 28853-C02-02, No. FIS2014-57026-REDT, No. FIS2014-51948-C2- 1-P, and No. FIS2014-51948-C2-2-P, and the Generalitat Valenciana in the program Prometeo II-2014/068.

[1] M. Bando, T. Kugo, S. Uehara, K. Yamawaki, and T. Yanagida, Phys. Rev. Lett. **54**, 1215 (1985).
[2] M. Bando, T. Kugo, and K. Yamawaki, Phys. Rep. **164**, 217 (1988).
[3] U. G. Meissner, Phys. Rep. **161**, 213 (1988).
[4] M. Harada and K. Yamawaki, Phys. Rep. **381**, 1 (2003).
[5] R. Molina, D. Nicmorus, and E. Oset, Phys. Rev. D **78**, 114018 (2008).
[6] L. S. Geng and E. Oset, Phys. Rev. D **79**, 074009 (2009).
[7] J. J. Xie, M. Albaladejo, and E. Oset, Phys. Lett. B **728**, 319 (2014).
[8] X. L. Ren, L. S. Geng, E. Oset, and J. Meng, Eur. Phys. J. A **50**, 133 (2014).
[9] R. Molina, H. Nagahiro, A. Hosaka, and E. Oset, Phys. Rev. D **80**, 014025 (2009).
[10] P. del Amo Sanchez *et al.* (*BABAR* Collaboration), Phys. Rev. D **82**, 111101 (2010).
[11] R. Aaij *et al.* (LHCb Collaboration), J. High Energy Phys. 09 (2013) 145.
[12] R. Aaij *et al.* (LHCb Collaboration), Phys. Rev. D **94**, 072001 (2016).
[13] P. Fernandez-Soler, Z. F. Sun, J. Nieves, and E. Oset, Eur. Phys. J. C **76**, 82 (2016).
[14] R. Akers *et al.* (OPAL Collaboration), Z. Phys. C **66**, 19 (1995).
[15] M. Moch (DELPHI Collaboration), Proc. Sci., HEP2005 (**2006**) 232.
[16] R. K. Mommsen, Nucl. Phys. B, Proc. Suppl. **170**, 172 (2007).
[17] T. Aaltonen *et al.* (CDF Collaboration), Phys. Rev. Lett. **100**, 082001 (2008).
[18] V. M. Abazov *et al.* (D0 Collaboration), Phys. Rev. Lett. **100**, 082002 (2008).
[19] R. Aaij *et al.* (LHCb Collaboration), Phys. Rev. Lett. **110**, 151803 (2013).
[20] F. K. Guo, P. N. Shen, H. C. Chiang, R. G. Ping, and B. S. Zou, Phys. Lett. B **641**, 278 (2006).
[21] F. K. Guo, P. N. Shen, and H. C. Chiang, Phys. Lett. B **647**, 133 (2007).
[22] A. Faessler, T. Gutsche, V. E. Lyubovitskij, and Y. L. Ma, Phys. Rev. D **77**, 114013 (2008).
[23] V. M. Abazov *et al.* (D0 Collaboration), Phys. Rev. Lett. **117**, 022003 (2016).

[24] R. Aaij *et al.* (LHCb Collaboration), Phys. Rev. Lett. **117**, 152003 (2016); **118**, 109904(E) (2017).
[25] A. M. Sirunyan *et al.* (CMS Collaboration), arXiv: 1712.06144.
[26] T. A. Aaltonen *et al.* (CDF Collaboration), arXiv: 1712.09620.
[27] V. M. Abazov *et al.* (D0 Collaboration), arXiv:1712.10176.
[28] W. Chen, H. X. Chen, X. Liu, T. G. Steele, and S. L. Zhu, Phys. Rev. Lett. **117**, 022002 (2016).
[29] S. S. Agaev, K. Azizi, and H. Sundu, Phys. Rev. D **93**, 074024 (2016).
[30] C. M. Zanetti, M. Nielsen, and K. P. Khemchandani, Phys. Rev. D **93**, 096011 (2016).
[31] Z. G. Wang, Commun. Theor. Phys. **66**, 335 (2016).
[32] L. Tang and C. F. Qiao, Eur. Phys. J. C **76**, 558 (2016).
[33] S. S. Agaev, K. Azizi, and H. Sundu, Eur. Phys. J. Plus **131**, 351 (2016).
[34] S. S. Agaev, K. Azizi, and H. Sundu, Phys. Rev. D **93**, 114007 (2016).
[35] Z. G. Wang, Eur. Phys. J. C **76**, 279 (2016).
[36] J. M. Dias, K. P. Khemchandani, A. Martnez Torres, M. Nielsen, and C. M. Zanetti, Phys. Lett. B **758**, 235 (2016).
[37] S. S. Agaev, K. Azizi, and H. Sundu, Phys. Rev. D **93**, 114036 (2016).
[38] S. S. Agaev, K. Azizi, and H. Sundu, Phys. Rev. D **93**, 094006 (2016).
[39] Y. R. Liu, X. Liu, and S. L. Zhu, Phys. Rev. D **93**, 074023 (2016).
[40] F. Stancu, J. Phys. G **43**, 105001 (2016).
[41] W. Wang and R. Zhu, Chin. Phys. C **40**, 093101 (2016).
[42] A. Ali, L. Maiani, A. D. Polosa, and V. Riquer, Phys. Rev. D **94**, 034036 (2016).
[43] X. H. Liu and G. Li, Eur. Phys. J. C **76**, 455 (2016).
[44] X. W. Kang and J. A. Oller, Phys. Rev. D **94**, 054010 (2016).
[45] Y. Jin, S. Y. Li, and S. Q. Li, Phys. Rev. D **94**, 014023 (2016).
[46] X. G. He and P. Ko, Phys. Lett. B **761**, 92 (2016).
[47] T. J. Burns and E. S. Swanson, Phys. Lett. B **760**, 627 (2016).
[48] R. Chen and X. Liu, Phys. Rev. D **94**, 034006 (2016).
[49] F. K. Guo, U. G. Meißner, and B. S. Zou, Commun. Theor. Phys. **65**, 593 (2016).
[50] Q. F. Lü and Y. B. Dong, Phys. Rev. D **94**, 094041 (2016).
[51] M. Albaladejo, J. Nieves, E. Oset, Z. F. Sun, and X. Liu, Phys. Lett. B **757**, 515 (2016).
[52] X. Chen and J. Ping, Eur. Phys. J. C **76**, 351 (2016).
[53] C. B. Lang, D. Mohler, and S. Prelovsek, Phys. Rev. D **94**, 074509 (2016).
[54] R. Albuquerque, S. Narison, A. Rabemananjara, and D. Rabetiarivony, Int. J. Mod. Phys. A **31**, 1650093 (2016).
[55] J. X. Lu, X. L. Ren, and L. S. Geng, Eur. Phys. J. C **77**, 94 (2017).
[56] B. X. Sun, F. Y. Dong, and J. L. Pang, Chin. Phys. C **41**, 074104 (2017).
[57] S. S. Agaev, K. Azizi, B. Barsbay, and H. Sundu, Eur. Phys. J. A **53**, 11 (2017).
[58] Z. Yang, Q. Wang, and U. G. Meißner, Phys. Lett. B **767**, 470 (2017).
[59] J. R. Zhang, J. L. Zou, and J. Y. Wu, Chin. Phys. C **42**, 043101 (2018).
[60] H. W. Ke and X. Q. Li, Eur. Phys. J. C **78**, 364 (2018).
[61] H. X. Chen, W. Chen, X. Liu, Y. R. Liu, and S. L. Zhu, Rep. Prog. Phys. **80**, 076201 (2017).
[62] E. Oset and A. Ramos, Eur. Phys. J. A **44**, 445 (2010).
[63] G. Ecker, J. Gasser, H. Leutwyler, A. Pich, and E. de Rafael, Phys. Lett. B **223**, 425 (1989).
[64] H. Nagahiro, L. Roca, A. Hosaka, and E. Oset, Phys. Rev. D **79**, 014015 (2009).
[65] S. Sakai, L. Roca, and E. Oset, Phys. Rev. D **96**, 054023 (2017).
[66] W. H. Liang, J. M. Dias, V. R. Debastiani, and E. Oset, Nucl. Phys. **B930**, 524 (2018).
[67] S. Okubo, Phys. Lett. **5**, 165 (1963).
[68] G. Zweig, in *Developments in the Quark Theory of Hadrons, Vol. 1*, edited by D. Lichtenberg and S. Rosen (Hadronic Press, Nonantum, MA, 1980), p. 22.
[69] J. Iizuka, Prog. Theor. Phys. Suppl. **37**, 21 (1966).
[70] J. A. Oller, E. Oset, and J. R. Pelaez, Phys. Rev. D **59**, 074001 (1999); **60**, 099906(E) (1999); **75**, 099903(E) (2007).
[71] W. H. Liang, C. W. Xiao, and E. Oset, Phys. Rev. D **89**, 054023 (2014).
[72] A. V. Manohar and M. B. Wise, *Heavy Quark Physics* (Cambridge University Press, Cambridge, England, 2000).
[73] C. Patrignani *et al.* (Particle Data Group), Chin. Phys. C **40**, 100001 (2016).